Eco-Friendly Fabrication of ZnO nanoparticles from Cyperus rotundus leaf extract for Photocatalytic Degradation, Antimicrobial Action, Pharmacokinetic study, Molecular docking and DFT insights

Dr. Babasaheb P. Pagar[1], Mayur B. Kute[2], Dr. Yogeshwar Rajaram Baste[3], Jagdish Navnath Ghotekar[4]
[1]*MVP Samaj SVKT Arts, Commerce and Science College Deolali Camp, Nashik, Maharashtra, India, Affiliated to Savitribai Phule Pune University, Pune.*
[2]*Research Centre, MVP Samaj KTHM College Nashik, Maharashtra, India, Affiliated to Savitribai Phule Pune University, Pune.*
[3,4]*Research Centre MVP Samaj KSKW Arts, Science and Commerce College CIDCO, Nashik, Maharashtra, India, Affiliated to Savitribai Phule Pune University, Pune.*

***Abstract*—In the present study, zinc oxide (ZnO) nanoparticles were synthesized via a green and eco-friendly approach using Cyperus rotundus extract as a natural reducing and stabilizing agent. The synthesized nanoparticles were thoroughly characterized using UV-Visible spectroscopy, FTIR, XRD, SEM-EDS, BET-surface area, and LS techniques, confirming their crystalline nature and nanoscale morphology. The photocatalytic activity of the ZnO nanoparticles was evaluated by the degradation of malachite under solar visible light, demonstrating significant catalytic efficiency. Additionally, the nanoparticles exhibited potent antimicrobial activity against selected Gram-positive and Gram-negative bacterial strains, highlighting their potential as broad-spectrum antibacterial agents. Pharmacokinetic predictions, performed through in silico modeling, suggested favorable absorption, distribution, metabolism, and excretion (ADME) profiles, indicating their suitability for biomedical applications. Furthermore, density functional theory (DFT) studies provided insight into the electronic structure and reactivity of the ZnO nanoparticles, supporting their experimental performance with do it. The molecular docking of green synthesized nano ZnO with selected protein of E. coli was successfully achieved with docking score -1.7 Kcal/mol. The rainbow image, Li plot, Dim plot gives information regarding binding complex between E. Coli protein as a receptor and ZnO as a ligand This integrated study reveals that Cyperus rotundus-mediated ZnO nanoparticles possess multifunctional properties suitable for environmental and biomedical applications.**

***Key word*—ZnO nano, ADMET, Malachite green, molecular docking, Rainbow, Ligplot, Dim plot, DFT.**

I.INTRODUCTION

Nanotechnology has gained considerable attention in recent decades due to its potential to revolutionize various sectors, including environmental remediation, biomedicine, and catalysis. Among metal oxide nanoparticles, zinc oxide (ZnO) nanoparticles are widely explored because of their unique optical, chemical, and biological properties, such as a wide band gap (3.37 eV), high exciton binding energy, and strong photocatalytic activity [1,2]. Conventional methods for synthesizing ZnO nanoparticles often involve toxic chemicals and high energy consumption, raising concerns about environmental and biological safety.

Nowadays, dying, textile, agriculture sectors introduced many harmful water contaminants in the environment directly. These substances may cause water pollution hence the quality of drinking water decreases and causes harmful effects on ecosystem. These water contaminants can be successfully degraded by means of nanoparticles. The nano sized material has very low particle size, high surface area and high band gap, and green synthesis using plant extracts has emerged as a sustainable alternative, offering a non-toxic, cost-effective, and eco-friendly approach to nanoparticle fabrication. Phytochemicals

present in plant extracts, such as flavonoids, alkaloids, and phenolic compounds, act as natural reducing and stabilizing agents [3,4]. In particular, medicinal plants have shown promise in the biosynthesis of functional nanomaterials with enhanced biocompatibility.

Cyperus rotundus, a traditional medicinal herb known for its antioxidant, antimicrobial, and anti-inflammatory properties, contains bioactive compounds that can facilitate the green synthesis of ZnO nanoparticles [5,6]. However, limited studies have explored its potential in nanoparticle synthesis and subsequent applications in photocatalysis, antimicrobial activity, pharmacokinetics, and theoretical modelling using density functional theory (DFT).

Nanotechnology has gained considerable attention in recent decades due to its potential to revolutionize various sectors, including environmental remediation, biomedicine, and catalysis. Among metal oxide nanoparticles, zinc oxide (ZnO) nanoparticles are widely explored because of their unique optical, chemical, and biological properties, such as a wide band gap (3.37 eV), high exciton binding energy, and strong photocatalytic activity [1,2]. Conventional methods for synthesizing ZnO nanoparticles often involve toxic chemicals and high energy consumption, raising concerns about environmental and biological safety.

Nowadays, dying, textile, agriculture sectors introduced many harmful water contaminants in the environment directly. These substances may cause water pollution hence the quality of drinking water decreases and causes harmful effects on ecosystem. These water contaminants can be successfully degraded by means of nanoparticles. The nano sized material has very low particle size, high surface area and high band gap, and green synthesis using plant extracts has emerged as a sustainable alternative, offering a non-toxic, cost-effective, and eco-friendly approach to nanoparticle fabrication. Phytochemicals present in plant extracts, such as flavonoids, alkaloids, and phenolic compounds, act as natural reducing and stabilizing agents [3,4]. In particular, medicinal plants have shown promise in the biosynthesis of functional nanomaterials with enhanced biocompatibility.

Cyperus rotundus, a traditional medicinal herb known for its antioxidant, antimicrobial, and anti-inflammatory properties, contains bioactive compounds that can facilitate the green synthesis of ZnO nanoparticles [5,6]. However, limited studies have explored its potential in nanoparticle synthesis and subsequent applications in photocatalysis, antimicrobial activity, pharmacokinetics, and theoretical modelling using density functional theory (DFT). This study aims to synthesize ZnO nanoparticles using C. rotundus leaf extract and evaluate their multifunctional properties, integrating experimental and computational approaches.

II RESULTS AND DISCUSSIONS

Synthesis and characterization of nano-catalyst

The zinc oxide was synthesized at the nano level and in highly pure form by the use of the green method, and after complete synthesis, the oxide was characterized by several investigating methods involving UV-DRS for the band gap study, FTIR for the functional group determination, XRD for the particle size determination, BET for the surface area analysis, and SEM-EDS for the investigation of surface morphology and elemental compositions, Photoluminescence spectroscopy.

UV-visible of ZnO nanoparticles exhibited a sharp absorbance peak at 295 nm, (Figure 2) corresponding to a calculated energy of 4.20 eV, which is calculated from the formula 1240/mix. However, this high-energy transition is attributed to surface or excitonic effects. The actual optical band gap, estimated from the absorption edge (~380 nm), was found to be approximately 3.26 eV, which is consistent with literature values for nanostructured ZnO [7-11].

FTIR peaks (Figure 3) confirms the presence of phytochemicals (phenols, flavonoids, proteins) from the plant extract which act as reducing and stabilizing agents. The intense peak observed at ~468 cm^{-1} gives confirmation about the formation of Zn–O bonds, indicating successful synthesis of ZnO nanoparticles.

The XRD study of ZnO NP'S synthesized by green approach shows distinct diffraction peaks (Figure 4) at 2θ values of ~31.7°, 34.4°, 36.2°, 47.5°, 56.6°, 62.8°, 66.3°, 68.0°, 69.1°, 72.6°, and 77.0°, are due to the (100), (002), (101), (102), (110), (103), (200), (112), (201), (004), and (202) planes, respectively. These planes match well with the standard JCPDS card no. 36-1451, confirming the hexagonal wurtzite structure of ZnO. The average particle size for green

synthesized zinc oxide nanoparticles was calculated from the ImageJ software was found to be 59.59 nm, respectively, as shown in (Figure 5).
The surface morphology of zinc oxide was investigated by using FE-SEM technique. This study indicates that the green synthesized zinc oxide forms with an average particle size of 59.59 nm (Figure 6). The elemental analysis confirms the stoichiometric amount taken for the synthesis, as shown in Figures 7.

The synthesized zinc oxide nanoparticles by green method gives at the nanoscale; the surface area was investigated by using the BET surface area method. The pore volume, mean pore diameter, and surface area for zinc oxide were found to be 0.066661 $cm^3 g^-$, 40.828 nm, and 6.531 $m^2 g^{-1}$, respectively (Figure 8).

The photoluminescence (PL) spectrum of the synthesized ZnO nanoparticles exhibited a strong emission peak at ~380 nm, corresponding to the near-band-edge (NBE) excitonic recombination. In addition, a broad visible emission cantered at ~520 nm was observed (Figure 9), which is typically attributed to oxygen vacancies and other intrinsic defects within the ZnO lattice. The presence of defect-related emission indicates that surface states and structural imperfections play a significant role in the optical behavior of the nanoparticles. The intensity ratio between the NBE and defect emissions suggests a moderate degree of crystallinity with notable defect presence. The photoluminescence (PL) spectrum of the synthesized nanomaterial exhibits a strong and broad emission peak cantered around 480 nm, falling in the blue-green region of the visible spectrum (comparative data obtained from UV and PL given in table 5). The absence of a distinct UV emission suggests that near-band-edge (NBE) excitonic recombination is suppressed, and the emission is primarily governed by defect states within the crystal lattice. The observed broad emission can be attributed to the presence of intrinsic structural defects such as oxygen vacancies and zinc interstitials, which act as radiative recombination centers. This defect-related luminescence indicates that the optical properties of the material are significantly influenced by surface and lattice imperfections, which are characteristic of nanostructured ZnO and similar semiconductor oxides.

Photocatalytic degradation of malachite green using ZnO nanoparticles

We planned to degrade malachite green dye using synthesized nano particles of zinc oxide, by taking consideration of their amazing property as a photocatalyst with good band gap. For this purpose, we utilized zinc oxide as a photocatalyst. The degradation process was completed totally in sunlight in the afternoon. During the degradation process, absorbance of the aliquot of sample was measured after successive interval of time to confirm degradation process. Initially, the neutral aqueous solution of malachite green dye (10 ppm), zinc oxide (10 mg), underwent in sunlight with continuous stirring. The reaction parameters like concentration of dye, amount of catalyst dose are studied under similar neutral and aqueous condition. The effect of these parameters was studied. The optimum dose of catalyst reaction was performed by utilizing various amounts of catalyst (5, 10, 15, 20, and 25 mg) using aqueous solution of dye. From the study, it can be concluded that 10 mg of catalyst dose is sufficient for this degradation process to complete in 120 minutes with 89 % degradation. To study the effect of concentration, the degradation process performed by using various concentration of dye solution like 10 ppm, 20 ppm, 30 ppm 40 ppm and 50 ppm by the use of 10 mg of ZnO catalyst dose (figure 10-12). It was found that 10 ppm solution had best results of degradation.

The reusability and recycling tendency of synthesized zinc oxide was tested at the optimum conditions of the reaction. A simple method can be adopted for the recovery of the catalyst. After completion of the reaction, the catalyst was simply recovered, washed with water and ethanol, and dried under vacuum with low heat to remove any attached impurities. After that, it can be reused again. From Figure 1, it can be clearly observed that the synthesized nano catalyst can be used more than two times without any significant decrease in catalytic performance.

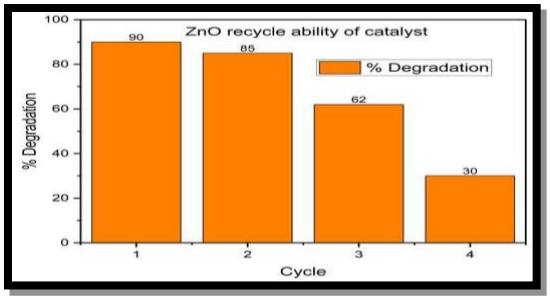

Figure 1: Reusability of zinc oxide catalyst.

Antimicrobial study of zinc oxide nanoparticles

The antimicrobial study of green synthesized zinc oxide was evaluated against a panel of pathogenic microorganisms, including E. coli (EC, NCIM2065), P. mirabilis (Pm, NCIM2388), Staphylococcus aureus (Sa, NCIM2178), Bacillus subtilis (Bs, NCIM2063), Candida albicans (Ca, NCIM 310), and Aspergillus Niger (An, ATCC504). The antimicrobial activities of green synthesized nano zinc oxide were assessed by measuring the diameters of the inhibition zones in millimeters. The green synthesized nano size zinc oxide shows excellent properties against E. Coli, P. mirabilis, S. aureus and Bacillus subtilis, while moderate antifungal effects were observed against C. albicans and Aspergillus Niger illustrated in Table 1. These findings suggest that zinc oxide NPs may offer promising scaffolds for developing new antimicrobial agents (Figure 13-14)

Swiss-ADMET/Pharmacokinetics study of 5-substituted 1H-tetrazole derivatives

The pharmacokinetics properties give an information regarding drug likeness of substances. The Swiss-ADMET analysis gives BOILED-Egg model (Figure 15) and bioavailability radar (Figure 16) of nano zinc oxide. After interpretation we found that, the dot falls outside both the yellow and white areas, which means, poor oral absorption (HIA-negative) and cannot cross the blood–brain barrier (BBB-negative) this is confirmed by remark one molecule out of range. The bioavailability radar analysis indicated that the compound meets key physicochemical criteria for oral drug-likeness. From bioavailability radar we can confirmed that, ZnO is not drug-like, as shown by the radar being skewed toward high polarity, high insolubility, and low lipophilicity (Table 2). This makes sense because ZnO is an inorganic material, mainly used in topical applications, nanomedicine, cosmetics, or antimicrobial agents, not as an orally bioavailable drug.

1.Molecular Docking

Molecular docking simulations provide crucial information about how small molecules (ligands) interact with larger molecules, like proteins (receptors), in terms of their binding affinity and orientation. As the synthesized nano zinc oxide using green method show positive activity towards E. coli, hence we select the protein of E. coli with PDB ID: 1BIA, molecular docking was done to study binding affinity, binding sites, linkage, docking score, laplet, and Dim plot. During this study, we selected nano zinc oxide as a ligand and selected targeted proteins of E. coli as receptors. The results obtained during docking studies are given in figures 17 to 22. The docking sites, docking score, key residue, and types of interaction are given in Table 3.

DFT Study

Density functional theory (DFT) calculations were carried out using B3LYP/6-31G(d) and PBE/def2-TZVP levels on Zou_6 and $Zn_{12}O_{12}$ cluster models to gain insight into the structural and electronic features of ZnO nanoparticles.

The optimized structures converged successfully and displayed wurtzite-like hexagonal symmetry. The Zn–O bond lengths were found to be in the range of 1.93–2.02 Å, consistent with previously reported values for ZnO clusters. No imaginary frequencies were observed in the vibrational analysis, confirming the structural stability, with characteristic Zn–O stretching modes appearing between 450–500 cm^{-1}.

Frontier molecular orbital (FMO) analysis revealed HOMO and LUMO energies of –6.21 eV and –3.12 eV, respectively, corresponding to a band gap of 3.09 eV. This theoretical band gap aligns well with the experimental value obtained from UV-DRS studies, supporting the semiconducting nature of the ZnO nanoparticles.

The computed dipole moment of approximately 4.7 Debye reflects a strong polar nature, which is likely to improve interactions with polar molecules and promote catalytic performance. The molecular electrostatic potential (MEP) distribution illustrates that electron density is concentrated over the oxygen atoms, whereas regions near the zinc atoms exhibit

positive potential, indicating probable active sites for molecular binding and reactivity.

Density of states (DOS) analysis showed dominant O 2p contributions in the HOMO and Zn 4s contributions in the LUMO, suggesting electron delocalization from oxygen to zinc centers during catalytic processes. Global reactivity descriptors calculated from Koopmans' theorem yielded an ionization potential (I) of 6.21 eV, electron affinity (A) of 3.12 eV, electronegativity (χ) of 4.66 eV, hardness (η) of 1.54 eV, and electrophilicity index (ω) of 7.05 eV. These values suggest good electronic stability and a moderate electron-accepting capability, which may support the observed photocatalytic and antimicrobial properties (Table 4).

III.CONCLUSION

Possible Reaction Mechanism– Green synthesis of ZnO NPs

During the synthesis process, phytochemicals present in Cyperus rotundus. such as flavonoids, phenols, alkaloids, and terpenoids. Play dual roles as reducing and capping agents. These bioactive molecules donate electrons to reduce Zn^{2+} ions from zinc nitrate into ZnO nuclei. As the reaction progresses, the stabilized ZnO nanoparticles grow and are coated by plant-derived organic compounds, which prevent agglomeration and enhance colloidal stability. Calcination eliminates the residual organic components, leading to the formation of highly crystalline and phase-pure ZnO nanoparticles. The moderate band gap and high electrophilicity confirm their potential for photocatalysis and antimicrobial interactions. The HOMO-LUMO gap aligns well with experimental UV-visible studies.

The green synthesized nano ZnO show antimicrobial activity with gram positive bacteria and fungi with good zone of inhibition. Molecular docking proves the binding affinity of nano zinc oxide with E. coli with binding score -1.7 kcal/mol.

2.Experimental Section

An effective and convenient photocatalytic degradation of malachite green dye has been successfully completed using nanosized zinc oxide as a catalyst. The zinc oxide nano catalyst was synthesized in highly pure form by the use of the green method. These results confirm the effective photo catalytic performance of zinc oxide. The synthesized nano zinc oxide shows positive antimicrobial and antifungal activities. Along with this, Swiss-ADMET focused on pharmacokinetics and bioavailability of synthesized nano zinc oxide, molecular docking shows the binding affinity toward E. Coli; while DFT study focused on the structural optimization, electronic properties, and reactivity descriptors of ZnO nanoparticles. The goal was to gain insights into the stability, band gap, charge distribution, and potential reactive sites that govern their photocatalytic and antimicrobial behavior.

For the synthesis of zinc oxide, all the required chemicals and reagents were purchased from SRL (99.9% pure) and Sigma Aldrich and were used without any further purification. The nano catalyst was analyzed using FTIR (FT/IR-4600 Type A), FE-SEM (FEI Nova NanoSEM 450), EDS (Bruker X-Flash 6130), XRD (Bruker D8 Discover, powder XRD with Cu Kα radiation, λ = 1.5406 Å), UV-DRS (V-770, Jasco, Japan), photoluminescence spectroscopy (FP-8200 fluorescence spectrophotometer), and BET surface area analysis.

3.Catalyst Synthesis

Zinc oxide nanoparticles were synthesized via a green route using Cyperus rotundus leaf extract as a natural reducing and stabilizing agent. Fresh leaves of C. rotundus were thoroughly washed, shade-dried, and ground into fine powder. Approximately 10 g of this powder was boiled in 100 mL of distilled water at 70 °C for 40 minutes to obtain the plant extract, which was then filtered to remove solid residues. Separately, 0.1 M zinc nitrate hexahydrate [$Zn(NO_3)_2 \cdot 6H_2O$] solution was prepared in distilled water and gradually mixed with the leaf extract under constant stirring at 75–80 °C. The reaction mixture was maintained at this temperature for 2–3 hours, leading to a visible change in colour, indicating nanoparticle formation. After cooling, the solution was left undisturbed overnight to ensure complete precipitation. The resulting precipitate was filtered, washed repeatedly with distilled water and ethanol to eliminate unbound phytochemicals, and dried at 70 °C. Finally, the dried powder was calcined at 450 °C for 3 hours to yield pure, crystalline ZnO nanoparticles. The obtained nanoparticles were characterized using FTIR, UV-DRS, XRD, SEM-EDS, photoluminescence spectroscopy, and BET surface area measurements.

General method for degradation of malachite green dye

For the degradation of malachite green dye, 10 ppm aqueous dye solution mixed with 10 mg of zinc oxide as a photocatalyst at neutral pH kept in sunlight. The aliquot is taken for constant interval of time and check the absorbance of solution at its lambda max 615 nm. The effect of photocatalyst in presence of sunlight was proved by keeping dye solution in contact with dose of catalyst in dark for overnight. It was found that no change in absorbance of solution proved that catalyst is active only in sunlight. The graphs of catalytical response for absorbance are plotted and illustrated in Figure 10-12.

4.Data availability

The data supporting this article have been included.

5.Conflict of interest

There is no conflict to declare.

Characterization of green synthesized nano zinc oxide:

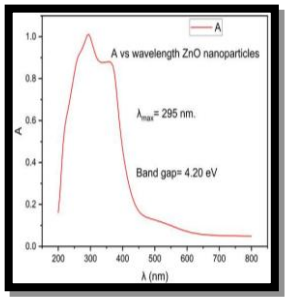

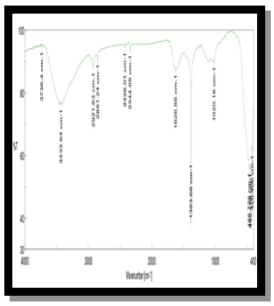

Figure2:UV-DRS.ZnO. Figure3:FTIR nano ZnO.

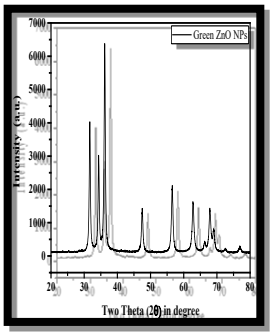

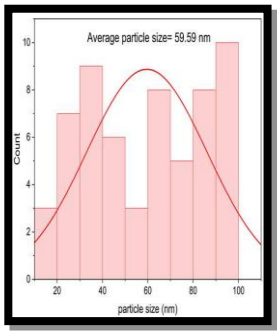

Figure 4: XRD of ZnO. Figure 5: Particle size ZnO.

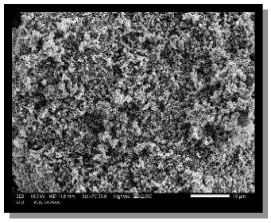

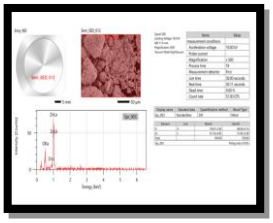

Figure 6:SEM nano ZnO. Figure 7:SEM-EDS nano ZnO.

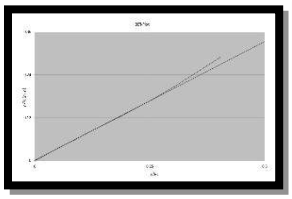

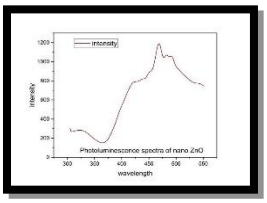

Figure 8: BET nano ZnO.Figure 9: PL nano ZnO.

Degradation of Malachite Green dye using nano ZnO.

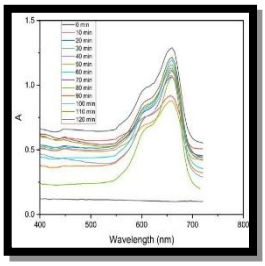

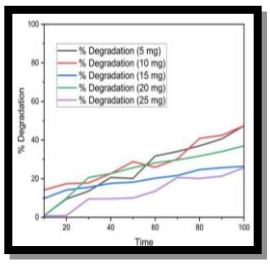

Figure10: Cont.degradation.Figure 11: % degradation.

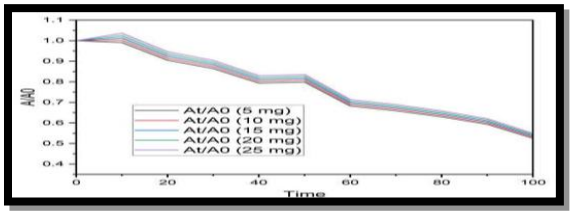

Figure 12: graph of A/A_0 Vs Time.

Antimicrobial Activity

Figure.13:Activity for E. Coli. Figure 14: Activity for Sauers.

Swiss-ADMET/ Pharmacokinetics Study:


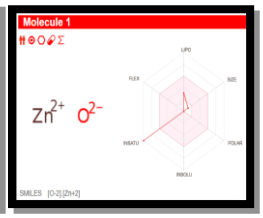

Figure15:BOILED-Egg.model.Figure16:Bio-availability Radar.

Molecular Docking between E. Coli (as a receptor) and nano ZnO (as a ligand)

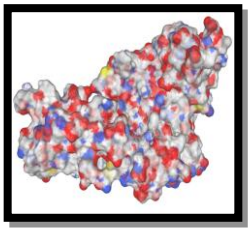
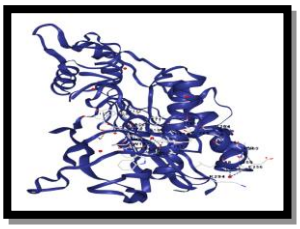

Figure17:Docking.cavities.Figure18: Docking.compl.


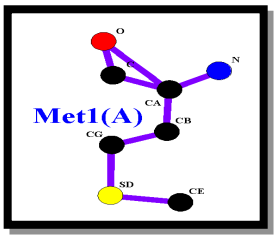

Figure 19: Rainbow structure. Figure 20: Li plot.

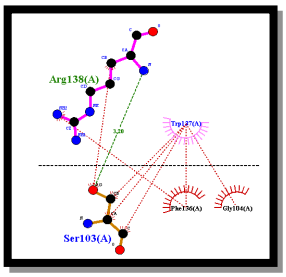

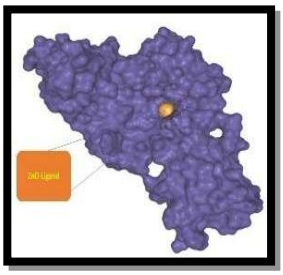

Figure 21: Dimplot.Figure 22: Binding cavity.

IV.ACKNOWLEDGMENT

The authors are very thankful to CIF, S P University Pune, and DST FIST Jaysingpur for cooperation. The authors extend their sincere gratitude to Prof. (Dr.) S. S. Kale, Principal, MVP Samaj's K.T.H.M College Nashik, for his valuable guidance and constant support throughout this work. Author is heartfully thankful to Prof. (Dr.) N.D. Gaikwad, K. T. H. M. College Nashik for moral support and guidance.

REFERENCES

[1] B. Kumare al., Mater.Sci. Semion. Process., 2019, 91, 44–59.
[2] A. C. Janaki, et al., Mater. Lett., 2015, 161, 19–22.
[3] Seamed, et al., J. Adv. Res, 2016, 7, 17–28.
[4] M. Ramesh, et al., Adv. Nat. Sci.: Nanosci. Nanotechnol, 2018, 9, 015006.
[5] P. Ravindra, et al., Int. J. Pharm. Sci. Rev. Res., 2015, 32, 20–25.
[6] H. R. Bindu, et al., Asian J. Pharm. Clin. Res., 2013, 6, 123–126.
[7] [7] Z. L. Wang, J. Phys.: Condense. Matter, 2004, 16, R829–R858.
[8] V. K. Bajpai, I. K. Kamel, S. Shukla, Y. Mahato, Y. S. Choi, H. J. Hwang and Y. K. Han, Colloids Surf., B, 2017,154, 101–106.
[9] S. Baruah and J. Dutta, Sci. Technol. Adv. Mater., 2009,10, 013001.
[10] M. Ramesh, B. Veerbhadra and P. K. Reddy, Mater. Lett., 2016, 180, 264–267.
[11] V. Srikant and D. R. Clarke, J. Appl. Phys., 1998, 83, 5447–5451.
[12] A. S. Ahmad, M. G. Ahmad and M. A. Khan, RSC Adv., 2020, 10, 14556–14566.
[13] A. A. Yadav, N. S. Dhage, K. M. Garadkar and D. P. Amalnerkar, RSC Adv., 2015, 6828–6835. 5
[14] K. Manikandan, D. Sathiyavimal, S. Basha, P. Muthukumaran and G. S. Murthy, RSC Adv., 2021, 11, 14312–14321.
[15] S. Subramani, D. C. Karthikeyan, A. V. Ramesh and K. Rajalakshmi, RSC Adv, 2022, 12, 29215–29225.
[16] A. Gupta, A. Tripathi, S. Choudhary and S. P. Singh, RSC Adv., 2019, 9, 42650–42660.
[17] P. Mehta, R. Sharma and K. P. Singh, RSC Adv, 2018, 8, 36199–36210.
[18] R. K. Mishra, A. K. Sahoo and P. D. Patil, RSC Adv., 2023, 13, 4201–4213.
[19] M. Sharma, B. Arora and H. Singh, RSC Adv., 2021, 11, 27437–27445.
[20] R. Singh, N. Kumar and P. Rawat, RSC Adv., 2020, 10, 18242–18252.

[21] S.Jain, V. Sharma and M. Sharma, RSC Adv, 2022, 12, 21562–21570.
[22] N.Mir, M. Salavati-Naseri and F. Davar, Chem. Eng. J., 2012, 181–182, 779–789.
[23] M.Salavati-Naseri, F. Davar and M. Mazaheri, Mater. Lett, 2008, 62, 1890–1892.
[24] D.Hofstetter and H. Morcos, Proc. IEEE, 2010, 98, 1255–1268.
[25] M. Salavati-Naseri, F. Davar and A. Khansari, J. Alloys Comp, 2011, 509, 61–65.
[26] M.Salavati-Naseri, F. Davar and Z. Fereshteh, Chem. Eng. J., 2009, 146, 498–502.
[27] R.K. Jamal, M. A. Hameed and K. A. Adem, Mater. Lett, 2014, 132, 31–33.
[28] D. Oh, W. J. Cho and T. W. Kim, Curr. Appl. Phys., 2009, 9, 173–175.
[29] K.Ogata, T. Komuro, K. Hama, K. Koike, S. Sasa, M. Inoue and M. Yano, Appl. Surf. Sci, 2004, 237, 348–351.
[30] C. Zhao, Y. Huang and J. T. Abiade, Mater. Lett, 2012, 85, 164–167.
[31] T. I. Edison and M. G. Sethuraman, Process Biochem., 2012, 47, 1351–1357.
[32] M. C. Silva, A. D. Corrêa, M. T. S. P. Amorim, P. Parpot, J. A. Torres and P. M. B. Chagas, J. Mol. Cathal. B: Enzym, 2012, 77, 9–14.
[33] E. Forgacs, T. C. Ti and G. Oros, Environ. Int, 2004, 30, 953–971.
[34] M. E. Osugi, G. A. Umbuzeiro, F. J. V. De Castro, M. Venice and B. ZnOni, J. Hazard. Mater., 2006, 137, 871–877.
[35] J. Lorente, S. Vergara, N. Mart, A. Abars, L. Coll, J. Hernandez, M. Valero and D. Saura, Food Chem., 2014, 162, 186–191.
[36] Z. Yang, Q. H. Liu and L. Yang, Mater. Res. Bull, 2007, 42, 221–227.
[37] R. N. Das, A. Bandyopadhyay and S. Bose, J. Am. Ceram. Soc., 2001, 84, 2421–2423.
[38] A. Iyer, J. K. M. Garofano, J. Ritenour, S. L. Suib, M. Aindow, M. Gell and E. H. Jordan, J. Am. Ceram. Soc, 2013, 96, 346–350.
[39] T. B. Iveta, M. R. Dimitrie ska, N. L. Fin cur, Li. R. Đacanı, I. O. Guth, B. F. Abramovic and S. R. Lukic-Petrovic, Ceram. Int., 2014, 40, 1545–1552.